



HAL
open science

Gas-phase rate coefficient of OH + cyclohexene oxide measured from 251 to 373 K

Hajar El Othmani, Yangang Ren, Wahid Mellouki, Véronique Daële, Max
Mcgillen

► **To cite this version:**

Hajar El Othmani, Yangang Ren, Wahid Mellouki, Véronique Daële, Max Mcgillen. Gas-phase rate coefficient of OH + cyclohexene oxide measured from 251 to 373 K. *Chemical Physics Letters*, 2021, 783, pp.139056. 10.1016/j.cplett.2021.139056 . insu-03352180

HAL Id: insu-03352180

<https://insu.hal.science/insu-03352180>

Submitted on 23 Sep 2021

HAL is a multi-disciplinary open access archive for the deposit and dissemination of scientific research documents, whether they are published or not. The documents may come from teaching and research institutions in France or abroad, or from public or private research centers.

L'archive ouverte pluridisciplinaire **HAL**, est destinée au dépôt et à la diffusion de documents scientifiques de niveau recherche, publiés ou non, émanant des établissements d'enseignement et de recherche français ou étrangers, des laboratoires publics ou privés.

1 **Gas-phase rate coefficient of OH + cyclohexene oxide measured from 251–373 K**

2 **Author list:**

3 Hajar El Othmani,^{1,2} Yangang Ren,¹ Abdelwahid Mellouki,¹ Véronique Daële,¹ Max R.
4 McGillen^{1*}

5 ¹ Institut de Combustion Aérothermique Réactivité et Environnement/OSUC–CNRS, 45071
6 Orléans, Cedex 2, France

7 ² Faculty of Science, Mohammed V University in Rabat, 10100 Rabat, Morocco

8 * corresponding author, email: max.mcgillen@cns-orleans.fr

9 **Target journal:**

10 *Chemical Physics Letters*

11 **Abstract:**

12 Absolute measurements of the rate coefficient of the title reaction are reported from 251–373
13 K using the laser-induced fluorescence–pulsed-laser photolysis technique, together with
14 room-temperature relative rate determinations using a simulation chamber. These are the first
15 reported values of this rate coefficient, which demonstrates a predominantly negative
16 temperature dependence that is more pronounced than with other epoxides, suggesting that
17 pre-reactive complexes contribute to the overall reactivity, and that these complexes are
18 comparatively stable for OH + cyclohexene oxide, which may result from its bicyclic
19 structure. This work provides new insights into the lesser-studied reactivity of the epoxide
20 functionality.

21 **Keywords:** epoxide, oxirane, hydroxyl, atmospheric chemistry, kinetics, rate constant

22
23 **1. Introduction**

24
25 There are many sources of epoxides in Earth’s atmosphere, both natural and anthropogenic.
26 Epoxides can be formed in the troposphere, mainly through the oxidation of alkenes. Some
27 epoxides are generated directly, from the reactions of alkenes with O₃ [1], NO₃ [2] and O(³P)
28 [3]. Whereas others can arise from the ring closure reactions of secondary radical species
29 formed from alkenes, such as the atmospherically important isoprene epoxydiols [4].

30 Epoxides may also be emitted directly to the atmosphere from floral scents [5], as well as
31 emissions being inferred from their various industrial applications [6].
32 Given the large global emission of olefinic precursor molecules, and the variety of these
33 unsaturated species, it is logical to expect that a large and diverse flux of epoxides enters the
34 atmosphere each year, and that knowledge of the atmospheric chemistry of epoxides is
35 required to understanding the total life-cycle of an alkene emission. Another potential source
36 of epoxides comes from the low-temperature combustion of hydrocarbons, which is known to
37 generate a variety of oxirane species [7].
38 Once they are released or formed in the troposphere, epoxides are expected to react with
39 radical species in the gas phase to form more oxidized species, or engage in acid-catalyzed
40 ring-opening reactions in the heterogeneous phase, forming low-volatility polyols [8]. The
41 competition between these processes will be defined by their respective reaction rates. At the
42 time of writing very few kinetic measurements are available for the oxidation of reactions of
43 epoxides with atmospheric oxidants such as OH or Cl [9], which limits our understanding of
44 the overall environmental fate of compounds possessing the epoxide functionality.
45 In this study, we report the rate coefficient of the following reaction over the temperature
46 range 251–373 K:

47



49

50 Cyclohexene oxide (1,2-epoxycyclohexane) is larger than those epoxides studied previously
51 [10–13], and, by virtue of the fact that it contains more C–H bonds than other epoxides found
52 in the kinetic database [9], is expected to react comparatively rapidly with OH and be lost
53 primarily through Reaction (1) under atmospheric conditions. The bicyclic structure of
54 cyclohexene oxide also contrasts with previously studied epoxides, and may influence its
55 reaction with OH. We will therefore discuss the reactivity of this molecule within the context
56 of other epoxides that have been studied so far.

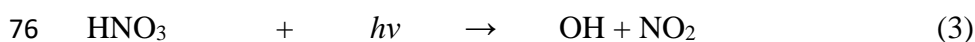
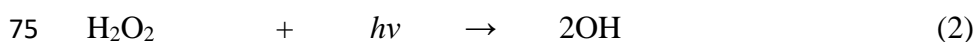
57 **2. Experimental methods**

58 Two complementary methods were used in this work to determine the kinetics of Reaction
59 (1). First, an absolute measurement, employing the pulsed-laser photolysis–laser-induced
60 fluorescence (PLP–LIF) technique to measure the rate coefficient as a function of
61 temperature. Second, a relative rate chamber method was used to measure the rate coefficient

62 at room temperature. The details of these measurements are described in the following
63 subsections.

64 **2.1 Absolute measurements using the PLP–LIF**

65 The PLP–LIF apparatus used in this work has been used in several previous studies, and will
66 be described only briefly here, for more details, please see these earlier publications [14,15].
67 The LIF reactor is a jacketed 200 cm³ Pyrex cell, with 4 quartz windows orthogonal to each
68 other. Heated/ cooled thermal transfer fluid (water or ethanol) was circulated through the outer
69 jacket in order to control the temperature of the gases inside the cell between 251 and 373 K.
70 Bath gas (He) pressures of ~100 Torr were used in all measurements, and were performed under
71 pseudo-first-order conditions such that [cyclohexene oxide] >> [OH]. OH radicals were
72 generated from the photolysis of precursor molecules using a 248 nm excimer laser operated at
73 10 Hz. To check for possible secondary interferences on OH decay profiles, two OH precursors
74 were used, H₂O₂ and HNO₃, which form OH through the following reactions:



77 Both of these precursors were introduced by sweeping over the headspace/ bubbling of liquid
78 samples with carrier gas (He). Given that both of these precursors have poor transmission
79 through mass flow controllers (MFCs), the flow of these precursors was controlled upstream
80 of the sample using an MFC. This leads to an uncertainty in the exact OH precursor
81 concentration, which we estimate instead, similar to previous work [16], using the following
82 equation:

$$83 [\text{OH precursor}] = k_d/k(T)_{\text{OH}}$$

84 where k_d represents the decay of OH in the absence of the cyclohexene oxide co-reactant, and
85 $k(T)_{\text{OH}}$ is the temperature-dependent reaction rate of OH with the OH precursor molecule in
86 question.

87 OH radicals were probed at 10 Hz using a frequency-doubled Nd:YAG pumped dye laser
88 tuned to the $A^2\Sigma^+ (v = 1) \leftarrow X^2\Pi (v = 0)$ transition near 282 nm. The resultant 308 nm
89 fluorescence was detected with a photomultiplier tube equipped with a bandpass filter
90 centered around 310 nm.

91 OH temporal decays were generated by varying the delay time between the photolysis and
92 probe pulses, thus changing the reaction time between OH and cyclohexene oxide. These

93 decays were found to abide by pseudo-first-order kinetics in each case, as described in the
94 following equation:

$$95 \ln\left(\frac{[\text{OH}]_t}{[\text{OH}]_0}\right) = \ln\left(\frac{S_t}{S_0}\right) = -(k[\text{cyclohexene oxide}] + k_d)t = -k't$$

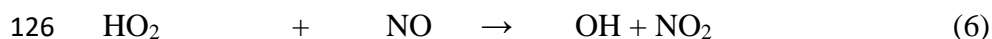
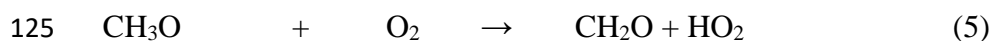
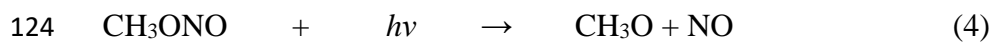
96 where the concentrations of OH, [OH], are proportional to fluorescence signal, S , at times 0
97 and t , respectively; and k' and k_d are first-order decay rates in the presence of and absence of
98 co-reactant cyclohexene oxide. k_d represents the decay of OH as a consequence of reactions
99 with OH precursors and diffusion out of the reaction volume, and was found to be exponential
100 over typical reaction times of 10,000 μs , and ranged from $\sim 70\text{--}500 \text{ s}^{-1}$ in our experiments. k'
101 ranged from $\sim 3000\text{--}50,000 \text{ s}^{-1}$, and was likewise found to be exponential under the
102 experimental conditions of this study. Rate coefficients, k , were determined from a weighted
103 linear least-squares fit to k' against [cyclohexene oxide].

104 To minimize experiment errors associated with co-reactant concentration, [cyclohexene
105 oxide] was monitored on-line using a multipass FTIR spectrometer, that was positioned
106 directly downstream of the LIF reactor. To be quantitative, the integrated band intensity was
107 determined as part of this work, and the band located between 2800 and 3100 cm^{-1} with an
108 integrated band intensity of $3.66 \times 10^{-17} \text{ cm molecule}^{-1}$ was used in our analyses (see Figures
109 S1 and S2 for further details).

110 **2.2 Relative measurements using a chamber apparatus**

111 To complement the absolute measurements, a simulation chamber was used as an independent
112 determination of the rate coefficient of Reaction (1). This system consists of a large PTFE
113 Teflon chamber equipped with *in situ* multipass FTIR and high-resolution time-of-flight
114 proton-transfer reaction mass spectrometry (PTR-ToF-MS) measurements. This apparatus has
115 been employed recently to measure the reaction rates of compounds of low volatility [17], and
116 is therefore considered to be a good additional test of kinetic determinations for potentially
117 surface-active chemicals such as an epoxide, that may be affected by the higher surface
118 area:volume ratios – as well as higher reactant and OH precursor concentrations –
119 encountered in the LIF reactor and its accompanying FTIR cell.

120 Measurements were conducted at $295 \pm 2 \text{ K}$, in an atmosphere of purified air in a 7.3 m^3
121 cuboidal chamber constructed of Teflon foil, described in detail elsewhere [18]. OH radicals
122 were generated from methylnitrite, photolyzed at 365 nm using $24 \times \text{UV-A T-40 L Viber-}$
123 Lourmat lamps in the following sequence of reactions:



127 A relative method was employed to determine the rate coefficient, by measuring the decay
 128 rate of [cyclohexene oxide] relative to that of a reference compound (1-propanol) with a
 129 known OH rate coefficient, $k_{\text{reference}}$. Comparison of these decays, taking into account dilution
 130 rate and wall-losses, k_d , yields the rate coefficient, k , through the following equation:

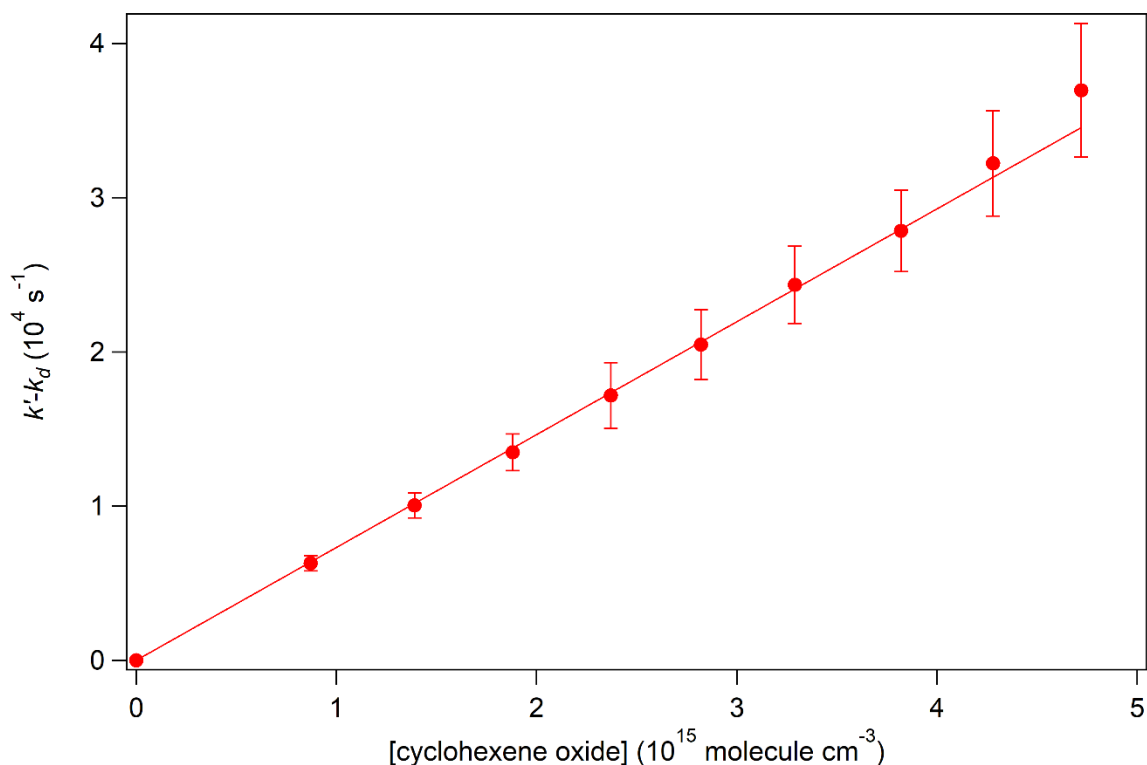
131
$$\ln\left(\frac{[\text{cyclohexene oxide}]_0}{[\text{cyclohexene oxide}]_t}\right) - k_d t = \frac{k_{\text{cyclohexene oxide}}}{k_{\text{reference}}} \ln\left(\frac{[\text{reference}]_0}{[\text{reference}]_t}\right) - k_d t$$

132 2.3 Materials

133 Cyclohexene oxide (>98%, Aldrich) was passed through several freeze-pump-thaw cycles
 134 prior to use. Helium carrier gas (Alphagaz 2, Air Liquide, 99.999%) was used as supplied in
 135 the PLP-LIF experiments. H_2O_2 (50 wt%, Alrich) was purified over the course of weeks with
 136 a slow flow of purified air. Gas-phase HNO_3 was taken from the headspace of a sample of
 137 70% redistilled HNO_3 , dehydrated by the dropwise addition of pure H_2SO_4 in a $\text{HNO}_3:\text{H}_2\text{SO}_4$
 138 ratio of 1:2 by volume, and maintained at 0°C in an ice bath. Methylnitrite was synthesized by
 139 dropwise addition of 50% H_2SO_4 in water into a stirred saturated solution of NaNO_2 in
 140 methanol, maintained at 0°C , the gaseous methylnitrite was then carried through a water
 141 bubbler and a u-tube containing P_2O_5 using a slow flow of nitrogen, and cold trapped at -
 142 196°C . 1- propanol (>99%, Aldrich) was used as supplied.

143 3. Results and discussion

144 Absolute measurements of the rate coefficient of Reaction (1) were measured using the PLP-
 145 LIF apparatus between 251 and 373 K in 100 Torr (He). Second-order plots of k' against
 146 [cyclohexene oxide] were of good quality in each case, with 2σ statistical errors between 2
 147 and 7%. An example of one of these plots is shown in Figure 1, and a summary of rate
 148 coefficient measurements together with experimental conditions is provided in Table S1.
 149 Total combined estimated uncertainties including cyclohexene oxide concentration (5%),
 150 pressure (2%) and temperature (2%) varied from 7–15%.

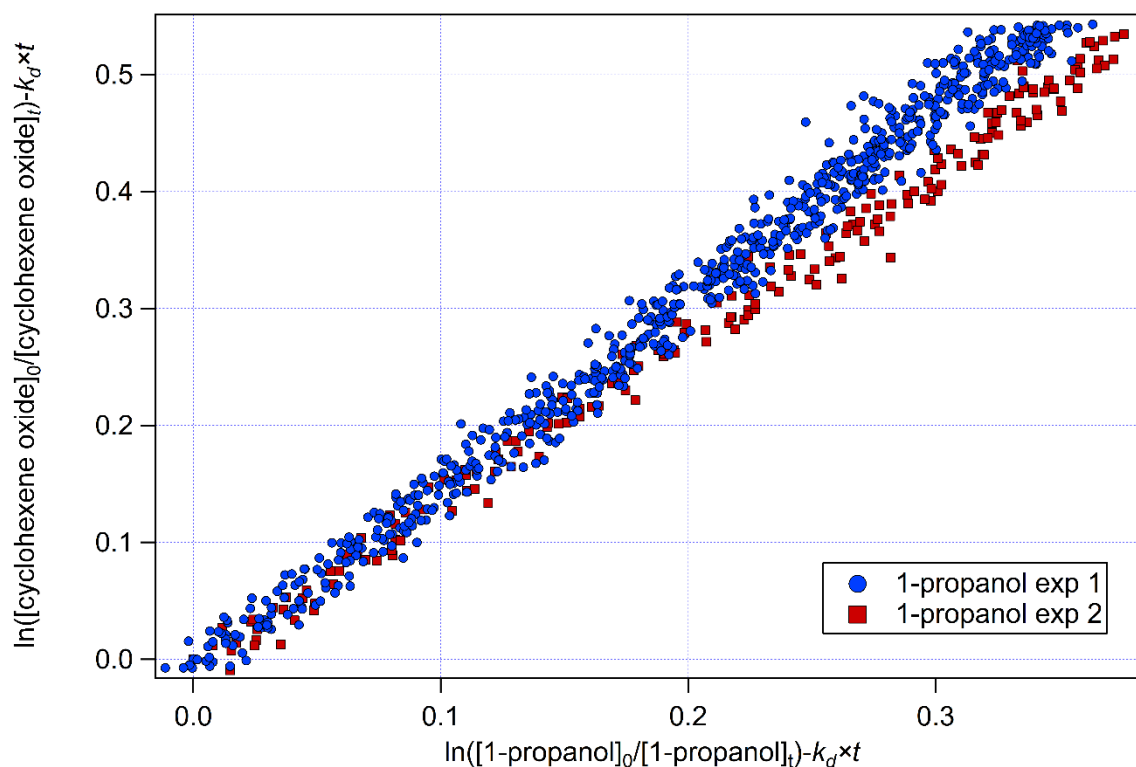


151

152 **Figure 1:** An example of a second-order plot measured at 274 K and 100 Torr (He).

153 Bimolecular rate coefficients are obtained from the slopes of error-weighted linear least-
 154 squares fits to data such as these.

155 The relative rate measurements at 295 K in an atmosphere of purified air using 1-propanol as
 156 a reference generated relative rate plots of high linearity and negligible intercept as shown in
 157 Figure 2. We made two separate determinations in this way, which were found to be self-
 158 consistent and also in excellent agreement with our absolute measurements. The consistency
 159 between the chamber and PLP–LIF measurements suggests that there is no strong pressure or
 160 bath gas dependence under our experimental conditions. Relative rate coefficient
 161 determinations are tabulated in Table S2. Total combined uncertainties for relative
 162 measurements were dominated by the absolute uncertainties in the 1-propanol reference rate
 163 coefficient, which is 5.86×10^{-12} cm^3 molecule $^{-1}$ s $^{-1}$ at room temperature, with estimated
 164 uncertainties of 10% [9].

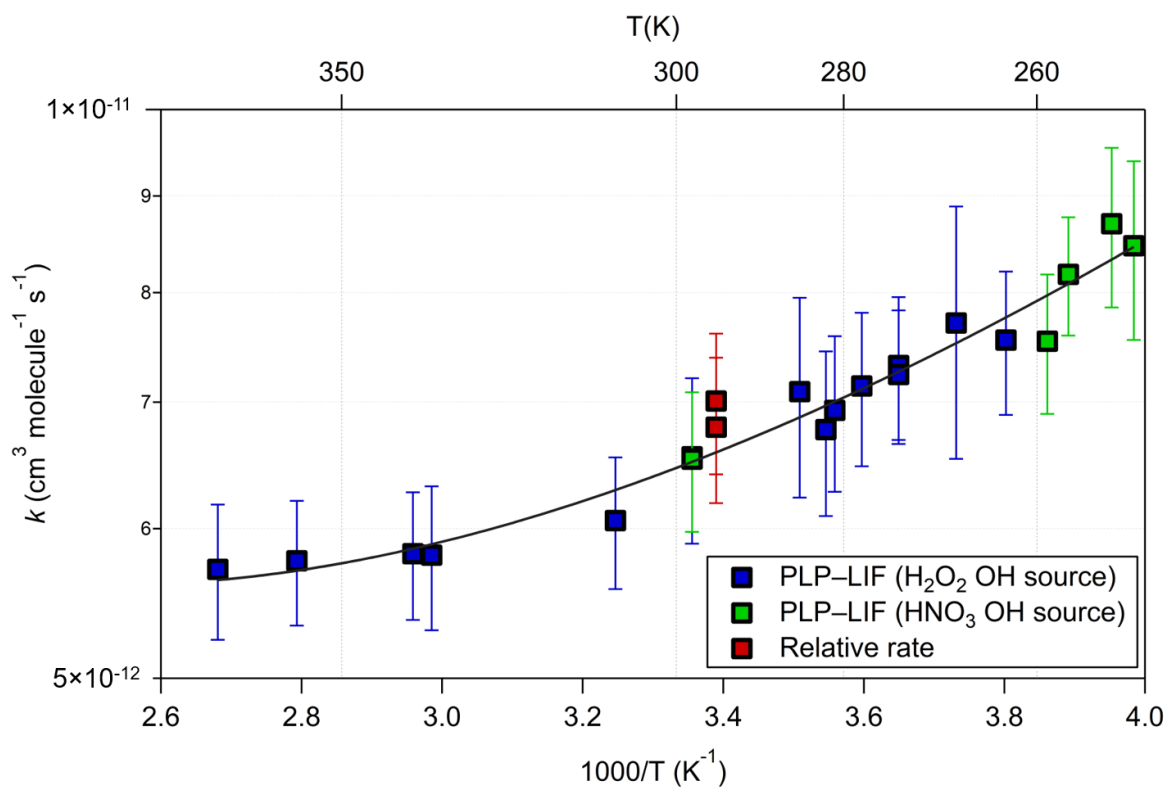


165

166 **Figure 2:** Relative rate experiments performed in a 7.3 m³ chamber, in which the decay of
 167 cyclohexene oxide is monitored using a PTR-ToF-MS alongside the reference compound, 1-
 168 propanol. Experiments 1 and 2 correspond to rate coefficient determinations of 7.01 ± 0.70 and
 169 6.79 ± 0.70 cm³ molecule⁻¹ s⁻¹ respectively.

170 There are no measurements available in the literature with which we can compare our current
 171 data, and the only gas-phase rate coefficient data for cyclohexene oxide known to this study is
 172 the reaction with atomic chlorine [19].

173 An Arrhenius diagram showing the dependence of the rate coefficient of Reaction (1) upon
 174 temperature is shown in Figure 3. A negative temperature dependence is observed, with some
 175 minor curvature towards the higher temperatures of this study.



176

177 **Figure 3:** Arrhenius diagram showing the temperature dependence of the rate coefficient of
 178 OH + cyclohexene oxide. Error bars represent the total combined uncertainties. The black line
 179 represents a modified Arrhenius fit to the data.

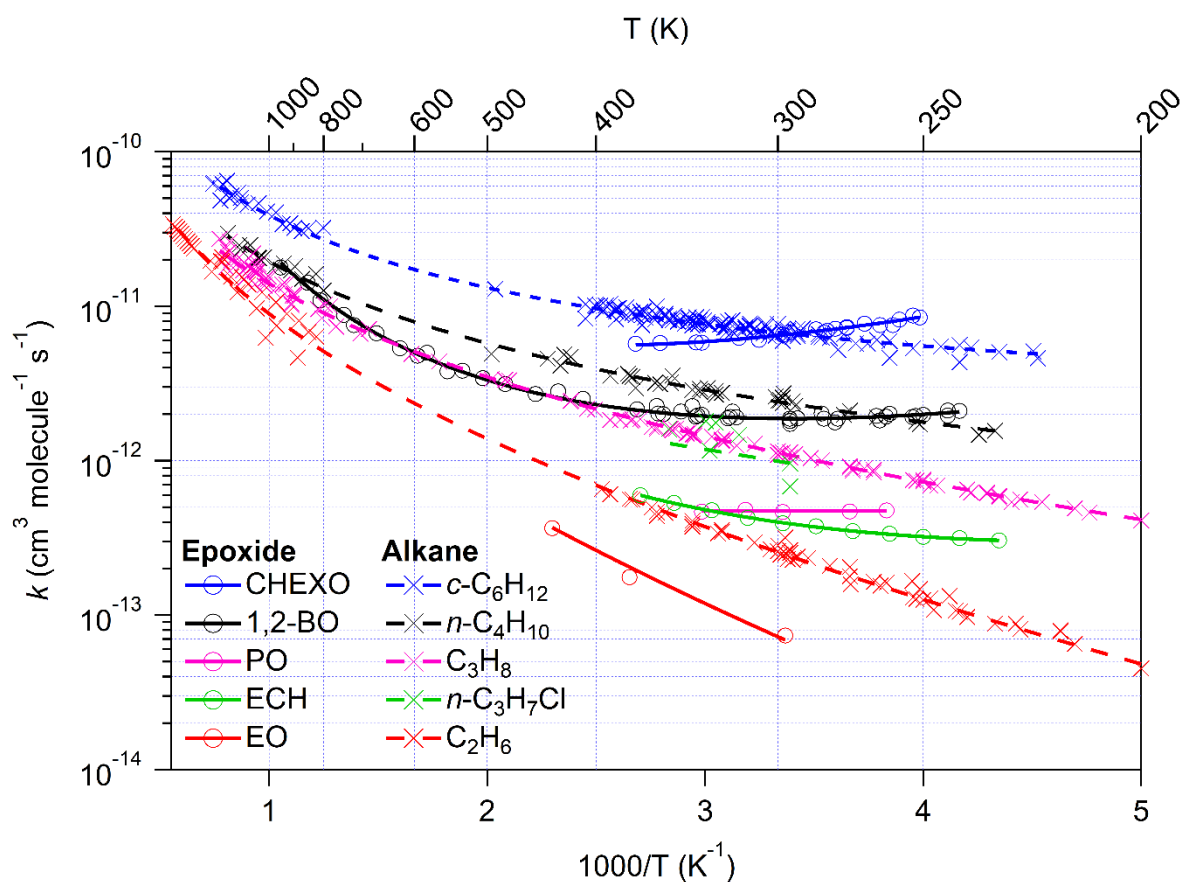
180 A modified Arrhenius expression was found to fit the data adequately over the temperature
 181 range of 251–373 K:

182

$$k_1 = 7.20 \times 10^{-14} \exp\left(\frac{1349}{T}\right) \left(\frac{T}{300}\right)^{3.4}$$

183 These results are qualitatively consistent with the reactions of OH with other epoxides as well
 184 as with other oxygenates, which tend to exhibit curvature and/ or negative temperature
 185 dependence below room temperature. This suggests, as discussed in case of 1,2-epoxybutane,
 186 that pre-reactive complexes may be facilitating these reactions at low temperatures [13]. What
 187 remains uncertain is to what extent these complexes enhance the overall rate coefficient when
 188 compared with the direct hydrogen abstraction mechanisms that are available to these
 189 molecules. To guide this discussion, we present the temperature dependence of a variety of
 190 epoxides together with their alkane analogs in Figure 4. From this diagram, it is apparent that
 191 for much of the atmospheric temperature range, epoxides tend to be less reactive than their
 192 corresponding alkane structure. As discussed by El Othmani et al. (2021) [13], this reduction

193 in reactivity is likely to relate to the increased bond dissociation energy of C–H bonds
 194 adjacent to the epoxide moiety. However, at lower temperatures, the OH rate coefficient of an
 195 epoxide can be larger than that of its alkane analog. This phenomenon can be explained by the
 196 increased stability of hydrogen-bonded van der Waals (vdW) complexes, which in turn
 197 increases the probability of quantum tunnelling in these reactions, as has been observed for
 198 other oxygenated molecules [20]. Besides this, there are other possibilities, such as the
 199 existence of a submerged barrier, a low barrier, or a barrierless reaction towards products. In
 200 such circumstances, quantum tunnelling may not contribute to the overall rate coefficient.
 201 Submerged and low barriers are encountered frequently under atmospheric conditions such as
 202 the electrophilic addition of OH to alkenes [21]. Low barriers are also observed in certain
 203 hydrogen abstraction reactions, especially where weak C–H bonds are present, as is the case
 204 of the reaction of OH + formaldehyde [22]. However, given that this is considered to be a
 205 hydrogen abstraction mechanism, and accounting for the fact that the presence of the oxirane
 206 functionality is calculated to increase bond strength in neighbouring C–H bonds [23], we
 207 favour the hypothesis that vdW complexes are enhancing the overall rate coefficient at low
 208 temperatures through quantum tunnelling.



209

210 **Figure 4:** A comparison between the temperature dependences of epoxides and their alkane
211 analogs. Epoxides are abbreviated as follows: CHEXO (cyclohexene oxide), 1,2-BO (1,2-
212 butylene oxide), PO (propylene oxide), ECH (epichlorohydrin), EO (ethylene oxide). All
213 kinetic data are taken from the database of McGillen et al. (2020) [9], except for the recent
214 data of El Othmani et al. [13].

215 The temperature at which the rate coefficient of the epoxide overtakes its alkane counterpart –
216 after some necessary extrapolation – appears to follow the order cyclohexene oxide > 1,2-
217 epoxybutane > propylene oxide > epichlorohydrin > ethylene oxide. This also follows the
218 order of decrease in the number of C–H bonds contained within each of these pairs.

219 Simultaneously, it can be seen that the proportion by which the rate coefficient is decreased
220 becomes less as the number of C–H bonds increases. This is intuitive, since the fraction of C–
221 H bonds adjacent to the epoxide (i.e. the least reactive sites) decreases as the total number of
222 C–H bonds grows, with the corollary being that, for larger epoxides, the reactivity would tend
223 towards that of the alkane analog.

224 Assuming that our hypothesis is valid, and that the overall rate coefficient is affected by
225 quantum tunnelling effects brought about by vdW complexes, the lifetime of the vdW
226 complex will affect the extent to which the rate coefficient is enhanced by tunnelling
227 processes. This lifetime increases as temperature (and kinetic energy) decreases. However,
228 there are several other factors that can influence this phenomenon. One example is the binding
229 energy of the complex, which will be largely dictated by the facility with which a molecule
230 forms hydrogen bonds with the OH radical co-reactant. Carboxylic acids, for example, form
231 particularly stable complexes, which reside in a potential energy well of $\sim 33 \text{ kJ mol}^{-1}$ [24],
232 and as a result, their OH rate coefficients tend to be large, with a pronounced negative
233 temperature dependence even at high temperatures [25]. A second factor is the entropic cost
234 of forming the vdW complexes. These tend to have a cyclic structure, and as a consequence,
235 have the capacity to shut down free rotors within molecules, which has been calculated to
236 affect the phenomenological rate coefficient under some conditions [26]. Cyclohexene oxide
237 is an interesting counterexample, in that it is purely cyclic to begin with, which should make
238 the formation of the vdW complex more favourable energetically, a second factor contributing
239 to this phenomenon is that the oxirane cycle is expected to be out-of-plane of the C_6 cycle,
240 which may facilitate the participation of the neighbouring CH_2 group in a vdW complex. Both
241 of which represent potential reasons why the onset of negative temperature dependence
242 occurs at a higher temperature for Reaction (1) than with other epoxides. A further effect may

243 come from an increase in the rate of vibrational relaxation that is afforded to molecules of a
244 larger size, which would explain why the reaction of OH with ethylene oxide shows no
245 negative temperature dependence within the temperature range that it has been studied so far
246 [10].

247 Other interpretations of the overall u-shaped Arrhenius profiles of the epoxides are possible,
248 for example, this would be anticipated from modified transition state theory in systems with
249 negative activation energies [27]. However, in the absence of high-level calculations, we
250 cannot assess whether or not this is a better explanation of our kinetic results compared with
251 the statistical complexes mentioned above.

252 **4. Conclusions**

253 We present the first reported absolute kinetic measurements of the gas-phase reaction of OH +
254 cyclohexene oxide as a function of temperature between 251 and 373 K. This work serves to
255 extend the overall knowledge on the reactivity of epoxides towards the OH radical. Our
256 results indicate that the presence of the epoxide moiety in cyclohexene oxide leads to an
257 enhancement of the rate coefficient compared with its alkane analog, cyclohexane. This
258 suggests that the dominant loss process for this epoxide will be with atmospheric oxidants
259 such as the OH radical, and that acid-catalyzed ring-opening reactions for larger, more
260 reactive epoxides such as this may be of less importance. Assuming a representative
261 tropospheric OH concentration of 2×10^6 molecule cm^{-3} , and a room temperature rate
262 coefficient for Reaction (1) of 6.51×10^{-12} cm^3 molecule $^{-1}$ s $^{-1}$, we estimate from the following
263 equation:

$$264 \quad \tau = \frac{1}{k[\text{OH}]}$$

265 that the tropospheric lifetime, τ , of cyclohexene oxide is approximately 1 day. As it becomes
266 oxidized, this bicyclic molecule is expected (by analogy to the atmospheric fate of cyclohexyl
267 peroxy/ cyclohexyl alkoxy radicals) to lead to ring-opened products [28]. These have an
268 increased capacity for forming multifunctional oxygenated species, which we expect can
269 contribute to secondary organic aerosol formation.

270 **Acknowledgements:**

271 This work is supported by Labex Voltaire (ANR-10-LABX-100-01) and the European
272 Union's Horizon 2020 research and innovation programme through the EUROCHAMP-2020

273 Infrastructure Activity under Grant Agreement No. 730997 and the Marie Skłodowska Curie
274 Actions Programme (690958-MARSU-RISE-2015). M.R.M. thanks Le Studium for their
275 support over the duration of this project.

276 **References:**

- 277 [1] R. Atkinson, S.M. Aschmann, J. Arey, E.C. Tuazon, Formation yields of epoxides and
278 O(³P) atoms from the gas-phase reactions of O₃ with a series of alkenes, *Int. J. Chem.*
279 *Kinet.* 26 (1994) 945–950. <https://doi.org/10.1002/kin.550260908>.
- 280 [2] I. Wängberg, I. Barnes, K.H. Becker, Product and Mechanistic Study of the Reaction of
281 NO₃ Radicals with α-Pinene, *Environ. Sci. Technol.* 31 (1997) 2130–2135.
282 <https://doi.org/10.1021/es960958n>.
- 283 [3] R.J. Cvetanović, Molecular Rearrangements in the Reactions of Oxygen Atoms with
284 Olefins, *Can. J. Chem.* 36 (1958) 623–634. <https://doi.org/10.1139/v58-088>.
- 285 [4] F. Paulot, J.D. Crouse, H.G. Kjaergaard, A. Kurten, J.M. St. Clair, J.H. Seinfeld, P.O.
286 Wennberg, Unexpected Epoxide Formation in the Gas-Phase Photooxidation of
287 Isoprene, *Science*. 325 (2009) 730–733. <https://doi.org/10.1126/science.1172910>.
- 288 [5] J.T. Knudsen, R. Eriksson, J. Gershenzon, B. Ståhl, Diversity and Distribution of Floral
289 Scent, *Bot. Rev.* 72 (2006) 1–120. [https://doi.org/10.1663/0006-](https://doi.org/10.1663/0006-8101(2006)72[1:DADOF5]2.0.CO;2)
290 [8101\(2006\)72\[1:DADOF5\]2.0.CO;2](https://doi.org/10.1663/0006-8101(2006)72[1:DADOF5]2.0.CO;2).
- 291 [6] H.Q. Pham, M.J. Marks, Epoxy Resins, in: Wiley-VCH Verlag GmbH & Co. KGaA (Ed.),
292 *Ullmanns Encycl. Ind. Chem.*, Wiley-VCH Verlag GmbH & Co. KGaA, Weinheim,
293 Germany, 2005: p. a09_547.pub2. https://doi.org/10.1002/14356007.a09_547.pub2.
- 294 [7] M.G. Christianson, A.C. Doner, M.M. Davis, A.L. Koritzke, J.M. Turney, H.F. Schaefer, L.
295 Sheps, D.L. Osborn, C.A. Taatjes, B. Rotavera, Reaction mechanisms of a cyclic ether
296 intermediate: Ethyloxirane, *Int. J. Chem. Kinet.* 53 (2021) 43–59.
297 <https://doi.org/10.1002/kin.21423>.
- 298 [8] E.C. Minerath, M.J. Elrod, Assessing the Potential for Diol and Hydroxy Sulfate Ester
299 Formation from the Reaction of Epoxides in Tropospheric Aerosols, *Environ. Sci.*
300 *Technol.* 43 (2009) 1386–1392. <https://doi.org/10.1021/es8029076>.
- 301 [9] M.R. McGillen, W.P.L. Carter, A. Mellouki, J.J. Orlando, B. Picquet-Varrault, T.J.
302 Wallington, Database for the kinetics of the gas-phase atmospheric reactions of organic
303 compounds, *Earth Syst. Sci. Data*. 12 (2020) 1203–1216. [https://doi.org/10.5194/essd-](https://doi.org/10.5194/essd-12-1203-2020)
304 [12-1203-2020](https://doi.org/10.5194/essd-12-1203-2020).
- 305 [10] K. Lorenz, R. Zellner, Rate Constants and Vinyloxy Product Yield in the Reaction OH +
306 Ethylene Oxide, *Berichte Bunsenges. Für Phys. Chem.* 88 (1984) 1228–1231.
307 <https://doi.org/10.1002/bbpc.198400053>.
- 308 [11] V.L. Orkin, V.G. Khamaganov, S.N. Kozlov, M.J. Kurylo, Measurements of Rate Constants
309 for the OH Reactions with Bromoform (CHBr₃), CHBr₂Cl, CHBrCl₂, and Epichlorohydrin
310 (C₃H₅ClO), *J. Phys. Chem. A*. 117 (2013) 3809–3818. <https://doi.org/10.1021/jp3128753>.
- 311 [12] A. Virmani, M.P. Walavalkar, A. Sharma, S. Sengupta, A. Saha, A. Kumar, Kinetic studies
312 of the gas phase reaction of 1,2-propylene oxide with the OH radical over a
313 temperature range of 261–335 K, *Atmos. Environ.* 237 (2020) 117709.
314 <https://doi.org/10.1016/j.atmosenv.2020.117709>.
- 315 [13] H. El Othmani, Y. Ren, Y. Bedjanian, S. El Hajjaji, C. Tovar, P. Wiesen, A. Mellouki, M.R.
316 McGillen, V. Daële, Gas-Phase Rate Coefficient of OH + 1,2-Epoxybutane Determined

- 317 between 220 and 950 K, ACS Earth Space Chem. (2021) acsearthspacechem.1c00050.
318 <https://doi.org/10.1021/acsearthspacechem.1c00050>.
- 319 [14] A. Mellouki, S. Téton, G. Laverdet, A. Quilgars, G. Le Bras, Kinetic studies of OH
320 reactions with H_2O_2 , C_3H_8 and CH_4 using the pulsed laser photolysis - laser induced
321 fluorescence method, J. Chim. Phys. 91 (1994) 473–487.
322 <https://doi.org/10.1051/jcp/1994910473>.
- 323 [15] Y. Ren, M. Cai, V. Daële, A. Mellouki, Rate coefficients for the reactions of OH radical
324 and ozone with a series of unsaturated esters, Atmos. Environ. 200 (2019) 243–253.
325 <https://doi.org/10.1016/j.atmosenv.2018.12.017>.
- 326 [16] M.R. McGillen, M. Baasandorj, J.B. Burkholder, Gas-Phase Rate Coefficients for the OH
327 + *n*-, *i*-, *s*-, and *t*-Butanol Reactions Measured Between 220 and 380 K: Non-Arrhenius
328 Behavior and Site-Specific Reactivity, J. Phys. Chem. A. 117 (2013) 4636–4656.
329 <https://doi.org/10.1021/jp402702u>.
- 330 [17] Y. Ren, M.R. McGillen, V. Daële, J. Casas, A. Mellouki, The fate of methyl salicylate in
331 the environment and its role as signal in multitrophic interactions, Sci. Total Environ.
332 749 (2020) 141406. <https://doi.org/10.1016/j.scitotenv.2020.141406>.
- 333 [18] F. Bernard, G. Eyglunet, V. Daële, A. Mellouki, Kinetics and Products of Gas-Phase
334 Reactions of Ozone with Methyl Methacrylate, Methyl Acrylate, and Ethyl Acrylate, J.
335 Phys. Chem. A. 114 (2010) 8376–8383. <https://doi.org/10.1021/jp104451v>.
- 336 [19] C.M. Tovar, A. Haack, I. Barnes, I.G. Bejan, P. Wiesen, Experimental and theoretical
337 study of the reactivity of a series of epoxides with chlorine atoms at 298 K, Phys. Chem.
338 Chem. Phys. 23 (2021) 5176–5186. <https://doi.org/10.1039/D0CP06033J>.
- 339 [20] D.E. Heard, Rapid Acceleration of Hydrogen Atom Abstraction Reactions of OH at Very
340 Low Temperatures through Weakly Bound Complexes and Tunneling, Acc. Chem. Res.
341 51 (2018) 2620–2627. <https://doi.org/10.1021/acs.accounts.8b00304>.
- 342 [21] J.P. Senosiain, S.J. Klippenstein, J.A. Miller, Reaction of Ethylene with Hydroxyl Radicals:
343 A Theoretical Study [†], J. Phys. Chem. A. 110 (2006) 6960–6970.
344 <https://doi.org/10.1021/jp0566820>.
- 345 [22] A. Zanchet, P. del Mazo, A. Aguado, O. Roncero, E. Jiménez, A. Canosa, M. Agúndez, J.
346 Cernicharo, Full dimensional potential energy surface and low temperature dynamics of
347 the $\text{H}_2\text{CO} + \text{OH} \rightarrow \text{HCO} + \text{H}_2\text{O}$ reaction, Phys. Chem. Chem. Phys. 20 (2018) 5415–
348 5426. <https://doi.org/10.1039/C7CP05307J>.
- 349 [23] P.C. St. John, Y. Guan, Y. Kim, B.D. Etz, S. Kim, R.S. Paton, Quantum chemical
350 calculations for over 200,000 organic radical species and 40,000 associated closed-shell
351 molecules, Sci. Data. 7 (2020) 244. <https://doi.org/10.1038/s41597-020-00588-x>.
- 352 [24] J. Mendes, C.-W. Zhou, H.J. Curran, Theoretical Chemical Kinetic Study of the H-Atom
353 Abstraction Reactions from Aldehydes and Acids by $\dot{\text{H}}$ Atoms and $\dot{\text{O}}\text{H}$, $\text{H}\dot{\text{O}}_2$, and $\dot{\text{C}}\text{H}_3$
354 Radicals, J. Phys. Chem. A. 118 (2014) 12089–12104.
355 <https://doi.org/10.1021/jp5072814>.
- 356 [25] V.G. Khamaganov, V.X. Bui, S.A. Carl, J. Peeters, Absolute Rate Coefficient of the OH +
357 $\text{CH}_3\text{C}(\text{O})\text{OH}$ Reaction at $T = 287\text{--}802$ K. The Two Faces of Pre-reactive H-Bonding, J.
358 Phys. Chem. A. 110 (2006) 12852–12859. <https://doi.org/10.1021/jp064922l>.
- 359 [26] C.-W. Zhou, J.M. Simmie, H.J. Curran, Rate constants for hydrogen-abstraction by O^{\cdot}H
360 from *n*-butanol, Combust. Flame. 158 (2011) 726–731.
361 <https://doi.org/10.1016/j.combustflame.2010.11.002>.
- 362 [27] L.N. Krasnoperov, J. Peng, P. Marshall, Modified Transition State Theory and Negative
363 Apparent Activation Energies of Simple Metathesis Reactions: Application to the

364 Reaction $\text{CH}_3 + \text{HBr} \rightarrow \text{CH}_4 + \text{Br}^\dagger$, J. Phys. Chem. A. 110 (2006) 3110–3120.
365 <https://doi.org/10.1021/jp054435q>.
366 [28] J. Platz, J. Sehested, O.J. Nielsen, T.J. Wallington, Atmospheric Chemistry of
367 Cyclohexane: UV Spectra of $\text{c-C}_6\text{H}_{11}^\bullet$ and $(\text{c-C}_6\text{H}_{11})\text{O}_2^\bullet$ Radicals, Kinetics of the Reactions
368 of $(\text{c-C}_6\text{H}_{11})\text{O}_2^\bullet$ Radicals with NO and NO_2 , and the Fate of the Alkoxy Radical $(\text{c-}$
369 $\text{C}_6\text{H}_{11})\text{O}^\bullet$, J. Phys. Chem. A. 103 (1999) 2688–2695. <https://doi.org/10.1021/jp984195x>.
370